expression, after some algebraic manipulation, is

$$\theta = \frac{|z_0|}{z_0}\tan^{-1}\left[\frac{a_e}{b_e}\frac{U-|A|}{\sqrt{4-(U-|A|)^2}}\right] \qquad z_0 \neq 0$$

$$= 0 \qquad z_0 = 0 \qquad (14)$$

where

$$U = \left[A^2 - B^2 + 1 - y + \frac{2|A|(B^2+1)}{\sqrt{y+1-B^2}}\right]^{1/2} + \sqrt{y+1-B^2}, \qquad (15)$$

$$y = [(1/27)(A^2+B^2-1)^3 + 2A^2B^2 + \sqrt{(4/27)A^2B^2(A^2+B^2-1)^3 + 4A^4B^4}\,]^{1/3} + [(1/27)(A^2+B^2-1)^3 + 2A^2B^2 - \sqrt{(4/27)A^2B^2(A^2+B^2-1)^3 + 4A^4B^4}\,]^{1/3} + 1/3(A^2+B^2-1)$$

with

$$A = \frac{b_e z_0}{a_e^2 - b_e^2} \quad \text{and} \quad B = \frac{a_e r_0}{a_e^2 - b_e^2}$$

Note that the above equation for θ is actually valid for $r_0 = 0$, i.e., for P on the polar axis; for in this case we find that $B = 0$, $y = A^2 - 1$, $U = 2 + |A|$, and so $|\theta| = \pi/2$.

Example

Using Fig. 1 it is quite easy to compute the geodetic altitude of P. Letting H denote this altitude, then

$$H = (|z_0| - b_e \sin t)\csc\theta$$

Since θ and t are related by Eq. (2) this last expression can be written in terms of t as

$$H = \left[\frac{|z_0| - b_e \sin t}{\sin t}\right][(1-e^2) + e^2 \sin^2 t]^{1/2}$$

where e is the eccentricity of the ellipse [Eq. (1)]. In terms of U in Eq. (15)

$$H = \left[\frac{2|z_0| - b_e(U-|A|)}{U-|A|}\right]\left[(1-e^2) + \frac{e^2}{4}(U-|A|)^2\right]^{1/2}$$

$$= r_0 - a_e \qquad z_0 \neq 0$$

$$z_0 = 0 \qquad (16)$$

Acknowledgments

Acknowledgment is given to Audrey Gioiello and Corine Turek for their help in the preparation of this paper. Space Applications Corporation, which provided the necessary funding for this Note, is also acknowledged.

References

[1] Berger, W.J. and Ricupito, J.R., "Geodetic Latitude and Altitude of a Satellite," *Journal of the American Rocket Society*, Vol. 1, Sept. 1960, pp. 901-902.

[2] Hart, W.L., *College Algebra*, D.C. Heath and Company, Boston, Mass., 1926, pp. 216-218, 236-239.

AIAA 82-4179

Gas Gun Study of Selected Buffers for Spall Fracture Reduction in Missile Materials

Willis Mock Jr.* and William H. Holt*
Naval Surface Weapons Center, Dahlgren, Va.

I. Introduction

A MISSILE warhead is usually located inside the outer skin or shroud part of a missile structure. After warhead detonation, the warhead fragments must penetrate the shroud to reach the target. The interaction of the fragments and shroud may cause decreased fragment velocity and fragment breakup. Recently a series of gas gun experiments was performed to study the effect of placing a polyethylene buffer material on the inside surface of the shroud to reduce fragment breakup.[1] The polyethylene thicknesses ranged from 1 to 9 mm. In the present investigation, 11 additional buffer materials have been studied. Experiments were performed for buffers in the 4-mm-thickness range. Composite specimens that simulated the shroud were impacted by steel disks. The impactor disks were soft recovered, sectioned, polished, and examined for fracture damage.

II. Experimental Techniques

A schematic of the muzzle region of the gas gun[2] with a target assembly containing a buffered composite specimen is shown in Fig. 1. A composite specimen consists of a wire harness layer, a 7075-T6 aluminum layer, a honeycomb layer, and another 7075-T6 aluminum layer. The projectile velocity is measured at impact with the three velocity pins. The steel impactor disk is supported only near its edge so the disk back surface is free over most of its area. The barrel is evacuated to minimize gas cushion effects on impact.

The impactor disks were fabricated from AISI C 1026 hot-rolled seamless tubing. The manufacturer's mechanical properties are 300-MPa yield strength, 540-MPa ultimate tensile strength, and 28% elongation. The measured impactor density was 7.83 Mg/m^3. The wire harness layer consisted of a series of parallel wires sealed between two thin plastic sheets. The honeycomb layer consisted of a plastic honeycomb material with a 0.072-Mg/m^3 density. Fast-setting epoxy was used to attach the four layers of a composite specimen together.

A gas gun shot was fired for each of the following buffer materials: Min-K 2000 molded insulation, polyrubber, polyurethane foam, silicone rubber, nylon, polyurethane, butyl rubber, polyester, neoprene, Micarta, and Melmac. The density of these materials ranges from 0.29 to 1.49 Mg/m^3. The average buffer thickness is 3.90 mm. The average impactor and specimen thicknesses are 9.1 and 9.4 mm, respectively. Average thickness values for the four specimen layers are as follows: 1.63-mm-thick wire harness layer, 1.61-mm-thick 7075-T6 aluminum layer, 5.41-mm-thick honeycomb layer, and 0.76-mm-thick 7075-T6 aluminum layer. The average diameter of the impactors and composite specimens is 29 mm.

A buffered specimen was secured inside a Lucite target holder with epoxy paste. The steel disks were soft recovered after impact to minimize any unintentional damage. The soft

Received Dec. 8, 1981; revision received Feb. 11, 1982.

*Research Physicist, Weapons Systems Department.

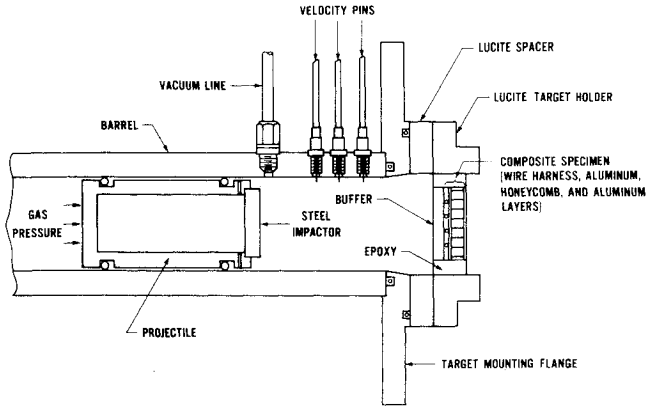

Fig. 1 Schematic of muzzle region of gas gun showing a steel impactor disk and buffered composite specimen.

recovery arrangement consisted of two bales of rags that were placed in the recovery box at the muzzle of the gas gun.

III. Results and Discussion

The gas gun recovery experiments are summarized in Table 1. The average impactor velocity was 0.88 km/s. The initial impactor stress was calculated for each shot using known Hugoniot equations of state[3-5] and the measured impactor velocity. It is expected that both elastic and plastic waves were generated in the steel impactor disks for these impact stresses. The spall fracture that occurred in the disks was produced by tensile stresses resulting from the interaction of rarefaction (decompression) waves. The results for the 3.43-mm-thick polyethylene buffer shot from Ref. 1 are included in Table 1 for comparison with the results of the present series of experiments.

A qualitative description of the disk fracture damage is given in Table 1. Photographs of the sectioned surfaces are shown in Fig. 2. Damage was limited to the central region of a disk due to stress relief wave effects at the disk edge. The initial impact stresses ranged from 0.94 to 5.0 GPa. Heavy fracture damage occurred for the 0.94-GPa Min-K 2000 buffer shot. The damage was centered about 6 mm from the disk impact surface. Medium fracture damage occurred for

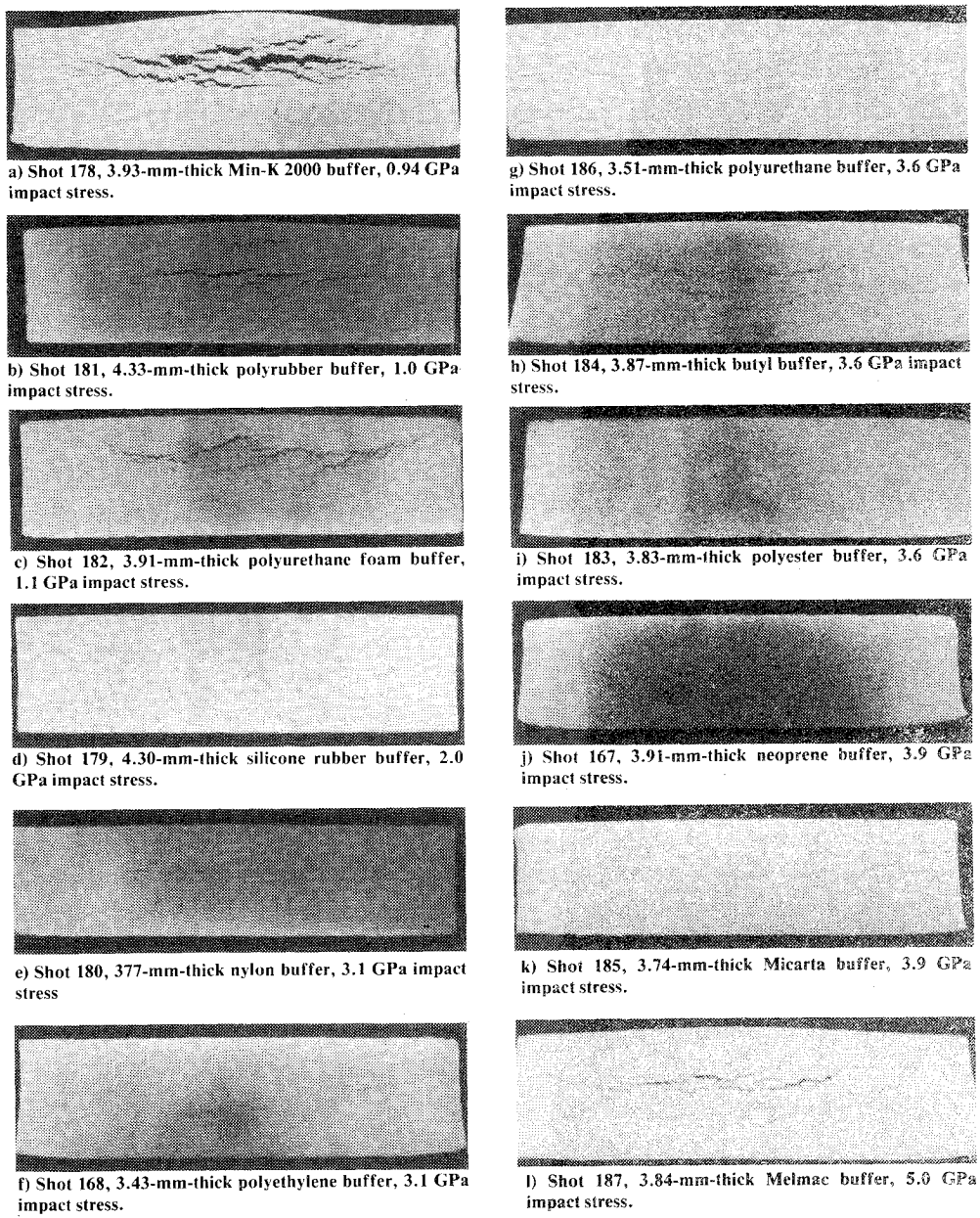

a) Shot 178, 3.93-mm-thick Min-K 2000 buffer, 0.94 GPa impact stress.

b) Shot 181, 4.33-mm-thick polyrubber buffer, 1.0 GPa impact stress.

c) Shot 182, 3.91-mm-thick polyurethane foam buffer, 1.1 GPa impact stress.

d) Shot 179, 4.30-mm-thick silicone rubber buffer, 2.0 GPa impact stress.

e) Shot 180, 377-mm-thick nylon buffer, 3.1 GPa impact stress

f) Shot 168, 3.43-mm-thick polyethylene buffer, 3.1 GPa impact stress.

g) Shot 186, 3.51-mm-thick polyurethane buffer, 3.6 GPa impact stress.

h) Shot 184, 3.87-mm-thick butyl buffer, 3.6 GPa impact stress.

i) Shot 183, 3.83-mm-thick polyester buffer, 3.6 GPa impact stress.

j) Shot 167, 3.91-mm-thick neoprene buffer, 3.9 GPa impact stress.

k) Shot 185, 3.74-mm-thick Micarta buffer, 3.9 GPa impact stress.

l) Shot 187, 3.84-mm-thick Melmac buffer, 5.0 GPa impact stress.

Fig. 2 Comparison of impactor fracture damage for the buffer materials. The disks are shown in order of increasing impact stress. The bottom edge of each disk is the impact surface.

Table 1 Summary of gas gun impact and soft recovery experiments

Shot no.	Impactor velocity,[a] km/s	Initial impactor stress,[b] GPa	Initial impactor thickness, mm	Final impactor thickness,[c] mm	Buffer material	Initial buffer thickness, mm	Qualitative description of impactor fracture damage
178	0.890	0.94	9.11	10.05	Min-K 2000	3.93	Heavy
181	0.867	1.0	9.10	9.31	Polyrubber	4.33	Medium
182	0.878	1.1	8.86	8.80	Polyurethane foam	3.81	Medium
179	0.879	2.0	9.06	8.85	Silicone rubber	4.30	Medium to light
180	0.863	3.1	9.12	8.93	Nylon	3.77	Light
168[d]	0.861	3.1	9.04	8.80	Polyethylene	3.43	Light
186	0.882	3.6	9.04	8.71	Polyurethane	3.51	Medium to light
184	0.882	3.6	9.11	8.84	Butyl rubber	3.87	Medium to light
183	0.883	3.6	9.06	8.76	Polyester	3.83	Light
167	0.878	3.9	9.04	8.76	Neoprene	3.91	Medium to light
185	0.886	3.9	9.04	8.77	Micarta	3.74	Medium to light
187	0.887	5.0	9.05	8.94	Melmac	3.84	Medium

[a]The estimated uncertainty is 1%. [b]The estimated uncertainty is 5-10%. The Hugoniot of Armco iron[3,4] was used since the 1026 steel Hugoniot was not available. The buffer material Hugoniots were obtained from Refs. 3 and 5. Since the Hugoniot for butyl rubber was not available, the polyurethane Hugoniot was used for shot 184. [c]Measured in the central region of the specimens. [d]Obtained from Ref. 1.

the 1.0-GPa polyrubber and the 1.1-GPa polyurethane foam buffer shots. For these shots the damage was centered about 5-6 mm from the disk impact surface. Medium-to-light or light fracture damage occurred for the eight shots in the 2.0-3.9-GPa stress range. (The light fracture damage occurred for impact stresses of 3.1 and 3.6 GPa.) The fracture damage was centered 3-5 mm from the disk impact surface for these eight shots. Medium fracture damage occurred about 4 mm from the disk impact surface for the 5.0-GPa Melmac buffer shot.

These results indicate that the buffer materials with shock impedances that produced impact stresses of about 1 and 5 GPa caused a larger amount of impactor fracture damage than the buffer materials with impact stresses between 2 and 4 GPa. The lower shock impedance buffers have densities between 0.29 and 0.91 Mg/m^3; the higher shock impedance buffer has a density of 1.49 Mg/m^3. The lower shock impedance materials probably provide inadequate spall protection for the impactor disk from the composite specimen. (Complete spall separation of an impactor disk occurred after it impacted an unbuffered composite specimen at 0.88 km/s.[1]) The higher shock impedance buffer material probably provides adequate spall protection for the impactor disk from the composite specimen but likely causes impactor fracture damage itself.

Acknowledgments

The authors would like to acknowledge W. G. Soper, D. C. Smith, and W. E. Elliott Jr. for their support and helpful discussions during this work.

References

[1]Mock, W. Jr. and Holt, W.H., "Gas Gun Study of Polyethylene Buffers for Spall Fracture Reduction in Missile Materials," *Journal of Spacecraft and Rockets*, Vol. 18, Nov.-Dec. 1981, pp. 565-566.

[2]Mock, W. Jr. and Holt, W.H., "The NSWC Gas Gun Facility for Shock Effects in Materials," Naval Surface Weapons Center, Dahlgren, Va., NSWC/DL TR-3473, July 1976.

[3]Kohn, B.J., "Compilation of Hugoniot Equations of State," Air Force Weapons Laboratory, Kirtland Air Force Base, N.Mex., AFWL-TR-69-38, April 1969.

[4]Barker, L.M., "α-Phase Hugoniot of Iron," *Journal of Applied Physics*, Vol. 46, June 1975, pp. 2544-2547.

[5]McQueen, R.G., Marsh, S.P., Taylor, J.W., Fritz, J.N., and Carter, W.J., "The Equation of State of Solids from Shock Wave Studies," *High Velocity Impact Phenomena*, edited by R. Kinslow, Academic Press, New York, 1970, pp. 293-417.

AIAA 82-4180

Visible Emission from Space Shuttle Main Engine Mach Disks

J. Wormhoudt* and V. Yousefian*
Aerodyne Research, Inc., Bedford, Mass.

Introduction

THE visible radiation from rocket plumes, observed in the form of (relatively easily obtained) photographs, can provide information about plume properties. This has led to studies estimating the visible emission intensity from rocket plumes,[1] considering several common radiation mechanisms.[2] In the absence of afterburning, a major cause of radiating plume features is reheating of the exhaust gas as it traverses the normal shocks (or Mach disks) which occur in both under- and overexpanded jets.

A widely observed example of such features are the Mach disk heated regions, which appear as pale blue inverted cones behind each of the three Space Shuttle main engine (SSME) nozzles (Fig. 1). However, the SSME propellants are pure H_2 and O_2, and therefore none of the visible radiation mechanisms described in Ref. 2 can be responsible for the observed radiation. It is the purpose of this Note to suggest a source for this radiation. This source is a continuum emission peaking in the blue which has previously been observed only in laboratory experiments with hydrogen flames, whose origin is still not known with certainty.

Properties Behind the Mach Disk

The plume gas properties downstream of the Mach disk are required to predict the radiation. These properties can be estimated using the assumption of frozen chemical composition from the nozzle exit until reheating by the normal shock. This is a reasonable assumption since in this region the characteristic flow time is short with respect to the chemical relaxation time. With the frozen chemistry assumption, the flow is isentropic between the nozzle exit and the upstream

Received Nov. 4, 1981; revision received Feb. 26, 1982.

*Senior Research Scientist, Applied Sciences Division.